Lateral septum neurotensin neurons link stress and anorexia

Estefania P. Azevedo[1], Bowen Tan[1], Lisa E. Pomeranz[1], Marc Schneeberger[1], Robert N. Fetcho[2], Katherine R. Doerig[1], Conor Liston[2], Jeffrey M. Friedman[1,3#], Sarah A. Stern[1*].

[1]Laboratory of Molecular Genetics, The Rockefeller University, New York, NY, 10065.

[2]Department of Psychiatry, Weill Cornell Medical College-New York Presbyterian Hospital, New York, NY, 10065

[3]Howard Hughes Medical Institute, The Rockefeller University, New York, NY, USA.

*Correspondence should be addressed to: sstern01@rockefeller.edu or friedj@mail.rockefeller.edu

Abstract

Anorexia Nervosa (AN) is an eating disorder characterized by severe voluntary food restriction[1]. Stress is known to be a precipitating factor in AN[2-5], but the underlying biology linking stress to feeding is not well understood. Here we describe a novel population of stress-responsive neurons in the lateral septum (LS) that express neurotensin (Nts^{LS}) and negatively regulate food intake. We used *in vivo* fiber photometry and chemo/optogenetics to show that Nts^{LS} neurons are activated by stressful experiences, including active escape in a predator-induced stress paradigm, and specifically decrease food intake in mice, without altering anxiety or locomotor behaviors. These neurons co-express Glp1r, and pharmacologic or genetic manipulations of Glp1r signaling in the LS recapitulate the behavioral findings shown using chemo/optogenetics. Finally, we mapped the outputs of Nts^{LS} neurons and show that activation of Nts^{LS} neuronal terminals in the lateral hypothalamus (LH) also decrease food intake. Taken together, these results show that NTS^{LS} neurons serve as a potential link between stress and anorexia and act by modulating hypothalamic pathways regulating feeding.

Voluntary food restriction, often to the point of starvation, is the canonical symptom of Anorexia Nervosa (AN), which has the highest mortality rate of any psychiatric illness[1]. Clinically, AN is often comorbid with depression, anxiety and stress disorders. Indeed, stress is considered to be a common precipitating factor in the pathogenesis of the disease[2-5]. In a recent report, we found that a projection from Drd2-expressing neurons in the hippocampus to the septal region reduces food intake[6]. Consistent with this, a prior study showed that inhibitory neurons in the lateral septum (LS) have been implicated in the modulation of appetite[7]. Because the LS is part of the anterior limbic system which regulates emotional behaviors, particularly stress, anxiety and aggression[8-9], we considered the possibility that this region might link stress to reduced food intake.

We first exposed mice to acute restraint stress and examined the pattern of c-fos within the LS. Consistent with previous experiments[10], restraint stress was associated with an increase in the number of c-fos+ cells in LS compared to controls (Fig. 1a, Student's t-test, $*p<0.05$). Restraint stress also led to a decrease in food intake for the ensuing 2 hours (Fig. 1b, Two-way ANOVA with Bonferroni post-hoc, $*p<0.05$, $***P<0.001$). Separate studies previously identified a subpopulation of Neurotensin-expressing (Nts) neurons in the LS[11], and modulation of hypothalamic Nts neurons regulates feeding[12-16]. Therefore, we hypothesized that these neurons might respond to stress, and thus, modulate food intake.

We first examined whether stress leads to activation of Nts^{LS} neurons and whether this accounted for the observed increase of c-fos activation in the LS. Mice were exposed to restraint stress and c-fos (read-out as Fos mRNA) and Nts co-expression was analyzed within the LS using *in situ hybridization*. Stressed mice showed significant colocalization of Fos and Nts within the LS compared to control non-stressed mice (Fig. 1c, Student's t-

test, *p<0.05). This was in large part to do an increase in Fos and a concomitant induction of Nts RNA during stress (Extended Data Fig 1a and b). We found that ~30% of stress-induced Fos neurons were Nts+, and that ~55% of Nts+ neurons were also positive for stress-induced Fos expression. We then tested whether activation of Nts neurons would lead to a decrease in food consumption. We injected an AAV encoding hM3Dq, the Gq-coupled excitatory DREADD (designer receptor exclusively activated by designer drugs), to Nts neurons in the LS of Nts-cre mice. Mice injected with clozapine-N-oxide (CNO), which binds to hM3Dq and induces neuronal depolarization, showed increased c-fos in the LS (Fig. 1d, Student's t-test, **p<0.01) and displayed a robust suppression of food intake compared to mice treated with CNO after injection of a cre-dependent mCherry AAV into NTS-cre mice as well as saline-injected mice expressing the DREADD (Fig. 1e, two-way ANOVA with Benferonni post-hoc, ***p<0.001; Extended Data Fig1c and d). Conversely, mice expressing the inhibitory hM4Di receptor in Nts neurons showed an increase in food intake after CNO injection compared to mCherry controls over 24h (Extended Data Fig 1e). Food intake was unchanged after saline-injection of mice expressing the inhibitory DREADD (Extended Data Fig 1f). Chronic stimulation (Fig. 1f) or inhibition (Extended Data Fig 1g) of Nts neurons for 3 days in the LS produced a sustained effect on food intake that was maintained for as long as CNO was given to mice (Two-way ANOVA with Bonferonni post-hoc, **p<0.01, ****p<0.0001). In stressful situations, even fasted mice will stop eating (Extended Data Fig 1h). We next asked whether activation of Nts^{LS} neurons would also suppress food intake in mice in energy deficit. To that end, we fasted mice overnight and measured food intake over 2h in Nts-Cre and littermate controls expressing hM3Dq and injected with CNO. Even when mice were in a state of energy deficit, we

observed a significant decrease in the food intake in Nts-cre mice after 2 hours of refeeding (Extended Data Fig 1i).

In order to better characterize how Nts neurons respond to stress, we next analyzed the activity of Nts^{LS} neurons using fiber photometry to optically record calcium signals in freely behaving mice[17] (Fig. 2a). We found an increase in the Ca^{+2} signal at both the beginning and end of a 1-minute period of restraint, where the mouse was being manually restrained by the experimenter. However, these neurons showed an increase in Ca^{+2} signal only when animals were actively struggling to escape from the restraint, and were silent when the animals were immobilized or had stopped struggling (Fig. 2b, Extended Data Fig 2a). We also observed activation of these neurons while animals struggled during a 1-minute tail suspension (Fig. 2c, Extended Data Fig 2b). We thus wondered whether Nts neurons were specifically activated by flight-induced stress e.g. a stressful situation where the animals has an ability to escape. We therefore exposed mice to a simulated predator using a remote-controlled robotic spider. We found that exposing the mice to the robotic spider in a predator-induced stress paradigm led to a similarly strong activation of Nts^{LS} neurons response that persisted until the mouse could escape into a designated "safe" nest area (Fig. 2d, Extended Data Fig 2c). Furthermore, when the nest was removed and mice were again exposed to the spider, there was an increase in Ca^{+2} fluorescence (Fig. 2e, Extended Data Fig 2d). In contrast, we did not find a temporal correlation between Ca^{+2} signals and feeding (Extended Data Fig 2e and f) or a change during locomotion or exploration in the absence of a "predator" (Extended Data Fig 2g and h). These data show that Nts^{LS} neurons are activated by stressful stimuli *in vivo,* particularly those for which flight is a viable strategy, and remain active until the animal is in an environment that is

perceived to be protected.

Because of the link between stress and Nts^{LS} activation, we tested the role of Nts^{LS} neurons in a variety of behavioral tasks that assess anxiety, and found no changes in open field thigmotaxis or locomotion (Extended Data Fig 3a-c), open-field with novelty (Extended Data Fig 3d), elevated plus maze behavior (Extended Data Fig 3e-h), or novelty-suppressed feeding (Extended Data Fig 3i) after Nts^{LS} activation. Thus, although Nts^{LS} neurons are activated by stressful situations that increase movement, their activation does not itself induce anxiety-like behaviors.

The LS expresses a number of peptides and peptide receptors aside from neurotensin. We therefore asked whether other peptides co-expressed with Nts might also control feeding. In order to characterize Nts^{LS} neurons, we used viral-TRAP to molecularly profile these neurons[18]. We expressed an adeno-associated virus expressing an eGFP-tagged ribosomal protein (AAV-Introvert-EGFPL10a) in Nts^{LS} neurons of Nts-cre mice and isolated polysomes by immunoprecipitation with an anti-GFP antibody (Fig. 3a). We then performed RNA-sequencing and identified several genes that were enriched in the polysome fraction including inhibitory interneuron markers *Cort* and *Sst*, as well as *Glp1r*, *Cartpt* and *Mc3r* (Fig. 3b, Supplementary Table 1). We confirmed the upregulation of these markers as well as *Gfp* and *Nts* and downregulation of glial markers *Gfap* and *Mal* within this population using qPCR (Fig. 3c). We found that ~80% of septal Nts neurons coexpress Vgat, a marker of GABAergic neurons, (Figure 3d, Students' t-test, *$p<0.01$) while ~70% of Nts^{LS} neurons expressed Glp1r. Sst is expressed in ~50%, Cartpt in ~40% and Mc3r in ~20% of the septal Nts^{LS} neurons (Fig. 3e-i).

Because Glp1r also negatively regulates feeding in various brain regions[19] and

showed the highest colocalization with Nts^{LS} neurons, we asked Glp1r could mediate the effect of stress on feeding behavior. Indeed, it has been shown prebiously that infusion of Exendin-9 (Ex9, a GLP1R antagonist) within the LS blocked the stress-induced decrease in food intake[20]. We found increased Fos expression in Nts^{LS} neurons co-expressing Glp1r after stress, with ~40% of Nts/Fos+ neurons co-expressing Glp1r (Fig. 3j, Students' t-test, **$p<0.01$). We also found that Exendin-4, a Glp1r agonist increased Fos+ expression in ~65% Nts^{LS} neurons co-expressing Glp1r (Fig. 3k, Two-way ANOVA with Bonferroni post-hoc, ***$p<0.0001$). Similar to Nts^{LS} activation, activation of Glp1r neurons within the LS with the exendin-4 agonist or the activating Gq DREADD resulted in a decrease in food intake over 24h (Fig. 3m-n, Extended Data Fig 4a-c, Two-way ANOVA with Bonferroni post-hoc, *$p<0.05$, ****$p<0.0001$). In contrast, gating of Mc3r (expressed in ~20% of septal Nts neurons) with a septal infusion of its agonist (y-msh), or activation of Cartpt or Sst neurons using the activating Gq DREADD in the relevant cre lines had no effect on food intake (Extended Data Fig 4d-f). Activation of these other septal populations (Extended Data Fig 4g-i) also had no effect in the elevated plus maze assay (Extended Data Fig 4j-l).

Finally, we mapped the projections of Nts^{LS} neurons that mediate the effect on food intake. We mapped the projection sites of these neurons in several ways including the use of a cre-dependent GFP reporter AAV expressed in the LS of NT-cre mice (Fig. 4a) and also by expressing a cre-dependent anterograde herpes simplex virus, H129ΔTK-TT, within the LS of Nts-cre mice (Fig. 4b). We found a strong projection to the lateral hypothalamus using either method (Fig. 4a and 4b). This same LS to LH projection was seen when mapping fibers from Glp1r-cre mice expressing a cre-dependent mCherry from

an AAV injected into the LS (Extended Data Fig 5a). The LH is a well-established site regulating food intake[21], and we then tested whether specific activation of the Nts^{LS} →LH projection would lead to a similar decrease in food consumption as activation of all of the septal Nts^{LS} cell bodies. We expressed a cre-dependent Chr2 virus within the LS of Nts-cre mice and implanted a fiber above the LH (Extended Data Fig 5b). Activation of this pathway with blue light led to an increase in c-fos in the LS and in the LH (Extended Data Fig 5c and d) and a significant decrease of food intake compared to controls expressing mCherry reporter, which reversed after light stimulation was removed (Fig. 4c, Two-way ANOVA with post-hoc Bonferroni correction, $*p<0.05$). Similar to the effect of activating the entire Nts^{LS} population of neurons, activation of the LH projecting Nts^{LS} neurons led to a ~50% decrease in food intake compared to controls. As before, no change in locomotion or anxiety related behaviors was observed (Extended Data Fig 5e-g).

Feeding is a complex motivated behavior and the elucidation of the neural mechanisms that control nutrient intake will provide a basis for understanding how other stimuli such as stress influence the behavior. The limbic region is classically known to regulate emotional and learned behaviors[22] including the response to stressful stimuli and its important role in regulating homeostatic behaviors such as feeding is just beginning to emerge. Anorexia nervosa is often triggered by stress and the delineation of the neural circuits linking feeding to stressful stimuli may provide a framework for better understanding the pathogenesis of this and other nutritional disorders.

The LS is part of the limbic system and the data reported here reveals a previously unknown role for neurotensin neurons co-expressing Glp1r, within the lateral septum to reduce food intake in response to stress. The data further indicate this effect is mediated by

a projection to the lateral hypothalamus. Prior studies have suggested that the LS is involved in active stress coping[23,24], and we find that Nts^{LS} neurons specifically respond during a stress situation, including a "predator induced stress paradigm but only under conditions in which flight (or movement) is an adaptive response. Since the functional consequence of this activation is to decrease food intake, this neural population may be related to coping mechanisms that dispense with voluntary food intake until appropriate countermeasures to mitigate the stressful event have been taken. Thus, this population of neurotensin neurons appears to play an integratory function and represents a link between stress and food intake, thus providing a novel entry for understanding how complex inputs - in this case food deprivation vs. danger - can compete to generate an adaptive response.

Together with recent data from our laboratory and others[6,25-26] (Azevedo 2019, Newmyer 2019, Land 2014), this suggests that higher order brain regions which project downstream can integrate information about the surrounding environment and provide powerful modulation of basal feeding circuits which ultimately control behavioral output.

Methods

Animals and breeding.

C57BL/6J (Stock# 000664), Nts-Cre (Stock# 017525), Sst-Cre (Stock# 028864), Cartpt-Cre (Stock# 028533), and Glp1r-cre (Stock# 029283) mice were obtained from Jackson Laboratories and housed according to the guidelines of the Rockefeller's University Animal Facility. Males and females at age 8-20 weeks were used throughout this study and all animal experiments were approved by the Rockefeller University IACUC, according to NIH guidelines. Male and female mice were used for Nts-cre, Sst-cre, Cartpt-Cre and

Glp1r-cre experiments. In experiments that used Cre+ and Cre- mice, littermates were used. No differences were determined based on gender. Mice were kept on a 12-h/12-h light/dark cycle (lights on at 7:00 a.m.) and had access to food and water ad libitum, except when noted otherwise. All feeding experiments used standard rodent chow pellets.

Stereotaxic Injections.

All AAVs used in this study were purchased from UNC Vector Core or Addgene, except where noted. AAV5-DIO-hM3Dq-mCherry or AAV5-DIO-Chr2-mCherry were used for activation studies. AAV5-DIO-hM4Di-mCherry was used for inhibition studies. Control AAV5-DIO-mCherry virus was used for comparison and for terminal projection mapping. AAV5-DIO-GCaMP6s was used for fiber photometry studies. AAV5-Introvert-GFPL10a was a gift from Alexander Nectow. H129ΔTK-TT virus was a gift from David Anderson and was used as described previously[27] (Mice were anesthetized with isoflurane, placed in a stereotaxic frame (Kopft Instruments) and bilaterally injected in the lateral septum using the following coordinates relative to bregma: AP: +0.1; ML: 0.0, DV: -3.00 (Paxinos). A total of 400 nL of virus at high titer concentrations (at least 10^{11}) were injected per site at a rate of 100 nL/min. For pharmacological experiments, cannula were implanted in the LS at the same coordinates as above. For fiber photometry experiments, optic fiber implants (Doric) were inserted at the same coordinates as above. For optogenetics experiments, optic fiber implants (Thor Labs) were implanted bilaterally over the LH at the following coordinates relative to bregma: AP: -1.80 mm; ML: + 1.50 mm, DV: -5.25 mm at a 10° angle (Paxinos). Implants were inserted slowly and secured to the mouse skull using two layers of Metabond (Parkell Inc). Mice were singly housed and monitored in the first weeks

following optic fiber implantation. For all surgeries, mice were monitored for 72h to ensure full recovery and two weeks later mice were used in experiments. Following behavioral procedures, mice were euthanized to confirm viral expression and fiber placement using immunohistochemistry.

Restraint Stress

Except where noted for fiber photometry studies, restraint stress consisted of 1 hour of immobilization in a decapicone (Braintree Scientific) in a separate room adjacent to the housing room. Mice were returned to their homecage following restraint for further food intake measurements or until euthanasia.

Fiber photometry

Mice were acclimated to patch cables for 5 min for 3 days before experiments. Analysis of the signal was done using fiber photometry system and processor (RZ5P) from TDT (Tucker-Davis Technologies), which includes the Synapse software (TDT). Post-recording analysis was performed using custom-written MATLAB codes. The bulk fluorescent signals from each channel were normalized to compare across animals and experimental sessions. The 405 channel was used as the control channel. GCaMP6s signals that are recorded at this wavelength are not calcium-dependent; thus, changes in signal can be attributed to autofluorescence, bleaching, and fiber bending. Accordingly, any fluctuations that occurred in the 405 control channels were removed from the 465 channel before analysis. Change in fluorescence (ΔF) was calculated as (465 nm signal − fitted 405 nm signal), adjusted so that a $\Delta F/F$ was calculated by dividing each point in ΔF by the 405-nm

curve at that time. Z-score, plot traces and colormaps were calculated for all experiments using MATLAB. Peak analysis to determine frequency and amplitude of the signals was done by determining the median average deviation (MAD) of the corrected/normalized data set and peaks were identified as events that exceeded the MAD by 2.91 deviations[28]. Behavioral variables were timestamped in the signaling traces via the real-time processor as TTL signals from Noldus (Ethovision) software. This allowed for precise determinations of the temporal profile of signals in relation to specific behaviors. Behaviors were tested as follows. First, we tested response to food. Mice were fasted overnight and then placed into a clean homecage with food pellets introduced 5 minutes later. Food approach and consumption were scored. We then tested restraint by manually restraining mice for 5 minutes. Tail suspension was conducted by suspending mice by their tails for 5 minutes, as described[29]. To examine the role of predator escape, mice were placed into an open field that contained a designated safe zone consisting of an acrylic "nest". After 5 minutes, a remote-controlled spider (Lattburg) was introduced into the open field and began to pursue the mouse at random intervals. After 10-15 minutes the nest was removed. We scored times when the mouse fled from the spider as well as the removal of the nest. Locomotion was scored during the first 5 minutes in the open field arena. All behavior was manually scored by a second investigator who did not conduct the photometry experiment.

Chemogenetic and Pharmacological Feeding Experiments.

For acute feeding, mice were single housed and injected with either saline or clozapine-N-oxide (CNO; Sigma) at 1 mg/kg intraperitoneally (i.p), exendin-4 (Tocris, 1 mg/mL), or y-msh (Tocris, 150 nM) directly into the lateral septum before the dark phase and cumulative

food intake and body weight was measured at selected time periods. For chronic feeding, mice were single or double injected (every 12h) with CNO or saline before dark phase and food intake and body weight were measured. For experiments that require fasting, mice were single caged and food was removed before dark phase (16-23h of fasting in total). Cumulative food intake at each time point was calculated for analysis.

Elevated Plus Maze

Mice were placed at the center of a cross-shaped, elevated maze in which two arms are closed with dark walls and two arms are open and allowed to explore for 10 min. Mice were injected with CNO (1mg/kg) 1h before testing. After, mice were returned to their homecage and the maze floor was cleaned in between subjects. All subjects were recorded using a camera and behavior (time spent in open and closed arms, distance and velocity) were analyzed using Ethovison 9.0 (Noldus).

Open Field / Open Field with Novelty

Mice freely explored an open field arena (28 x 28 cm), divided into center and border regions, for 5 min. The time spent (in seconds) in the center area, were taken as measures of anxiety. To increase the anxiolytic nature of the task, a novel object was placed into the center of the arena (open field with novelty). Mice were injected with CNO (1mg/kg) 1h before testing. After, mice were returned to their homecage and the maze floor was cleaned in between subjects. All subjects were recorded using a camera and behaviors (time spent in center and border, distance and velocity) were analyzed using Ethovison 9.0 (Noldus).

Optogenetics Feeding Experiment.

Mice were previously habituated to patch cables for 3 days before experiments. Implanted optic fibers were attached to a patch cable using ceramic sleeves (Thorlabs) and connected to 473 nm laser (OEM Lasers/OptoEngine). Laser output was verified at start of each experiment. Blue light was generated by a 473 nm laser diode (OEM Lasers/OptoEngine) at 5-10 mW of power. Light pulse (10 ms) and frequency (10Hz) was controlled using a waveform generator (Keysight) to activate NT+ terminals in lateral hypothalamus. Animals were sacrificed to confirm viral expression and fiber placement using immunohistochemistry. Each feeding session lasted 80 min and it was divided in 1 trial of 20 min to allow the animal to acclimate to the cage and 3 trials of 20 min each (1h feeding session). During each feeding session, light was off during the first 20 min, on for 20 min and off again for the remaining 20 min. Consumed food was recorded manually before and after each session. To facilitate measurement, 3 whole pellets were added to cups and food crumbs were not recorded. Feeding bouts were recorded using a camera and the Ethovision 9.0 software (Noldus).

Viral-Trap (V-Trap)

Affinity purification of EGFP-tagged polysomes was done 3 or 4 weeks after virus injections, according to Nectow et al., 2017[18]. Briefly, mice were separated into 3 biological replicate groups of 4-6 mice per group and euthanized. Brains were removed, and the lateral septum was dissected on ice and pooled. Tissue was homogenized in buffer containing 10 mM HEPES-KOH (pH 7.4), 150 mM KCl, 5 mM MgCl2, 0.5 mM DTT, 100 µg/mL cycloheximide, RNasin (Promega) and SUPERase-In™ (Life Technologies) RNase

inhibitors, and Complete-EDTA-free protease inhibitors (Roche) and then cleared by two-step centrifugation to isolate polysome-containing cytoplasmic supernatant. Polysomes were immunoprecipitated using monoclonal anti-EGFP antibodies (clones 19C8 and 19F7; see Heiman et al., 2008[30]) bound to biotinylated-Protein L (Pierce; Thermo Fisher Scientific)-coated streptavidin-conjugated magnetic beads (Life Technologies). A small amount of tissue RNA was saved before the immunoprecipitation (Input) and both input and immunoprecipitated RNA (IP) were then purified using RNAeasy Mini kit (QIAGEN). RNA quality was checked using an RNA PicoChip on a bioanalyzer. RIN values >7 were used. Experiments were performed in triplicates for each group. cDNA was amplified using SMARTer Ultralow Input RNA for Illumina Sequencing Kit and sequenced on an Illumina HiSeq2500 platform.

RNA sequencing and qPCR analysis

RNA sequencing raw data was uploaded and analyzed using BaseSpace apps (TopHat and Cufflinks; Illumina) using an alignment to annotated mRNAs in the mouse genome (UCSC, Mus musculus assembly mm10). The average immunoprecipitated (IP) and Input value of each enriched and depleted genes with a q-value lower than 0.05 were plotted using GraphPad Prism (GraphPad). To validate the RNA Sequencing data, qPCR using predesigned Taqman probes (idtDNA) were used and cDNA was prepared using the QuantiTect Reverse Transcription Kit (Life Technologies). The abundance of these genes in IP and Input RNA was quantified using Taqman Gene Expression Master Mix (Applied Biosystems). Transcript abundance was normalized to beta-actin. Fold of Change were calculated using the ΔΔCt method.

Immunohistochemistry, quantifications and imaging.

Mice were perfused and brains were postfixed for 24h in 10% formalin. Brain slices were taken using a vibratome (Leica), blocked for 1h with 0.3% Triton X-100, 3% bovine serum albumin (BSA), and 2% normal goat serum (NGS) and incubated in primary antibodies for 24h at 4ºC. Then, free-floating slices were washed three times for 10 min in 0.1% Triton X-100 in PBS (PBS-T), incubated for 1h at room temperature with secondary antibodies, washed in PBS-T and mounted in Vectamount with DAPI (Southern Biotech). Antibodies used here were: anti-c-fos (1:500; Cell Signaling), anti-mCherry (1:1000; Abcam) goat-anti-rabbit (Alexa 488 or Alexa 594, 1:1000; Molecular Probes), goat anti-chicken Alexa488 or Alexa594 (1:1000; Molecular Probes). Images were taken using Axiovert 200 microscope (Zeiss) or LSM780 confocal (Zeiss) and images were processed using ImageJ software (NIH)[31]. C-fos counts were conducted for 3 or more sections / animal and averaged for each animal for statistical analysis.

Fluorescent In Situ Hybridization

For examination of gene expression and Fos experiments, tissue samples underwent single molecule fluorescent in situ hybridization (smFISH). Isoflurane anesthetized mice were decapitated, brain harvested and flash frozen on aluminum foil on dry ice. Brains were stored at −80°C. Prior to sectioning, brains were equilibrated to −16°C in a cryostat for 30 min. Brains were cryostat sectioned coronally at 20 μm and thaw-mounted onto Superfrost Plus slides (25x75 mm, Fisherbrand). Slides were air-dried for 60 to 90 min prior to storage at −80°C. smFISH for all genes examined— *Fos* (ACDBio Cat# 316921), *Nts* (ACDBio

Cat #420441), *Sst* (ACDBio Cat# 404631), *Glp1r* (ACDBio Cat # 418851), *Cartpt* (ACDBio Cat #432001), *Mc3r* (ACDBio Cat# 412541) - was performed using RNAscope Fluorescent Multipex Kit (Advanced Cell Diagnostics) according to the manufacturer'. Slides were counterstained for the nuclear marker DAPI using ProLong Diamond Antifade mounting medium with DAPI (ThermosFisher). Sections were imaged using an LSM780 confocal (Zeiss) and processed using ImageJ software. Counts were conducted for 2 or more sections/animal and averaged for each animal for statistical analysis.

Statistics

All results are presented as mean ± s.e.m. and were analyzed with Prism software or with Matlab. No statistical methods were used to predetermine sample sizes, but our sample sizes are similar to those reported in previous publications. Normality tests and F tests for equality of variance were performed before choosing the statistical test. Unless otherwise indicated, for feeding experiments we used a two-way ANOVA with Bonferroni correction to analyze statistical differences. $P < 0.05$ was considered significant (*$P < 0.05$, **$P < 0.01$, ***$P < 0.001$, ****$P<0.0001$). Image quantifications were analyzed using unpaired Students' t-tests. Fiber photometry data were analyzed using paired Students' t-tests. Animals in the same litter were randomly assigned to different treatment groups and blinded to experimenters in the various experiments. Injection sites and viral expression were confirmed for all animals. Mice showing incorrect injection sites or optic fiber placement were excluded from the data analysis.

References

1. Arcelus, J., Mitchell, A. J., Wales, J. & Nielsen, S. Mortality rates in patients with anorexia nervosa and other eating disorders. A meta-analysis of 36 studies. Arch. Gen. Psychiatry 68, 724–731 (2011).

2. Deep, A. L., Nagy, L. M., Weltzin, T. E., Rao, R. & Kaye, W. H. Premorbid onset of psychopathology in long-term recovered anorexia nervosa. Int. J. Eat. Disord. 17, 291–297 (1995).

3. Sharan, P. & Sundar, A. S. Eating disorders in women. Indian J. Psychiatry 57, S286–95 (2015).

4. Ruggiero, G. M., Levi, D., Ciuna, A. & Sassaroli, S. Stress situation reveals an association between perfectionism and drive for thinness. Int. J. Eat. Disord. 34, 220–226 (2003).

5. Naumann, E., Svaldi, J., Wyschka, T., Heinrichs, M. & von Dawans, B. Stress-induced body dissatisfaction in women with binge eating disorder. J. Abnorm. Psychol. 127, 548–558 (2018).

6. Azevedo, E. P. et al. A Role of Drd2 Hippocampal Neurons in Context-Dependent Food Intake. Neuron 102, 873–886.e5 (2019).

7. Sweeney, P. & Yang, Y. An Inhibitory Septum to Lateral Hypothalamus Circuit That Suppresses Feeding. J. Neurosci. 36, 11185–11195 (2016).

8. Anthony, T. E. et al. Control of Stress-Induced Persistent Anxiety by an Extra-Amygdala Septohypothalamic Circuit. Cell 156, 522–536 (2014).

9. Wong, L. C. et al. Effective Modulation of Male Aggression through Lateral Septum to Medial Hypothalamus Projection. Current Biology 26, 593–604 (2016).

10. Kubo, T. et al. The lateral septal area is involved in mediation of immobilization

stress-induced blood pressure increase in rats. Neurosci. Lett. 318, 25–28 (2002).

11. Lein, E. S. et al. Genome-wide atlas of gene expression in the adult mouse brain. Nature 445, 168–176 (2007).

12. Brown, J. A., Woodworth, H. L. & Leinninger, G. M. To ingest or rest? Specialized roles of lateral hypothalamic area neurons in coordinating energy balance. Front. Syst. Neurosci. 9, 9 (2015).

13. Goforth, P. B., Leinninger, G. M., Patterson, C. M., Satin, L. S. & Myers, M. G., Jr. Leptin acts via lateral hypothalamic area neurotensin neurons to inhibit orexin neurons by multiple GABA-independent mechanisms. J. Neurosci. 34, 11405–11415 (2014).

14. Leinninger, G. M. et al. Leptin action via neurotensin neurons controls orexin, the mesolimbic dopamine system and energy balance. Cell Metab. 14, 313–323 (2011).

15. Opland, D. et al. Loss of neurotensin receptor-1 disrupts the control of the mesolimbic dopamine system by leptin and promotes hedonic feeding and obesity. Mol Metab 2, 423–434 (2013).

16. Li, J. et al. An obligatory role for neurotensin in high-fat-diet-induced obesity. Nature 533, 411–415 (2016).

17. Gunaydin, L. a. et al. Natural neural projection dynamics underlying social behavior. Cell 157, 1535–1551 (2014).

18. Nectow, A. R. et al. Rapid Molecular Profiling of Defined Cell Types Using Viral TRAP. Cell Rep. 19, 655–667 (2017).

19. Kanoski, S. E., Hayes, M. R. & Skibicka, K. P. GLP-1 and weight loss: unraveling the diverse neural circuitry. Am. J. Physiol. Regul. Integr. Comp. Physiol. 310, R885–95 (2016).

1 20. Terrill, S. J., Maske, C. B. & Williams, D. L. Endogenous GLP-1 in lateral septum
2 contributes to stress-induced hypophagia. Physiol. Behav. 192, 17–22 (2018).
3 21. Stuber, G. D. & Wise, R. A. Lateral hypothalamic circuits for feeding and reward.
4 Nat. Neurosci. 19, 198–205 (2016).
5 22. LeDoux, J. E. Emotion circuits in the brain. Annu. Rev. Neurosci. 23, 155–184
6 (2000).
7 23. Singewald, G. M., Rjabokon, A., Singewald, N. & Ebner, K. The modulatory role of
8 the lateral septum on neuroendocrine and behavioral stress responses.
9 Neuropsychopharmacology 36, 793–804 (2011).
10 24. Bondi, C. O. et al. Noradrenergic facilitation of shock-probe defensive burying in
11 lateral septum of rats, and modulation by chronic treatment with desipramine. Prog.
12 Neuropsychopharmacol. Biol. Psychiatry 31, 482–495 (2007).
13 25. Newmyer, B. A. et al. VIPergic neurons of the infralimbic and prelimbic cortices
14 control palatable food intake through separate cognitive pathways. JCI Insight 5, (2019).
15 26. Land, B. B. et al. Medial prefrontal D1 dopamine neurons control food intake. Nat.
16 Neurosci. 17, 248–253 (2014).
17 27. Lo, L. & Anderson, D. J. A Cre-dependent, anterograde transsynaptic viral tracer for
18 mapping output pathways of genetically marked neurons. Neuron 72, 938–950 (2011).
19 28. Calipari, E. S. et al. In vivo imaging identifies temporal signature of D1 and D2
20 medium spiny neurons in cocaine reward. Proc. Natl. Acad. Sci. U. S. A. 113, 2726–2731
21 (2016).
22 29. Can, A. et al. The tail suspension test. J. Vis. Exp. e3769 (2012).
23 30. Heiman, M. et al. A translational profiling approach for the molecular

characterization of CNS cell types. Cell 135, 738–748 (2008).

31. Schneider, C. A., Rasband, W. S. & Eliceiri, K. W. NIH Image to ImageJ: 25 years of image analysis. Nat. Methods 9, 671–675 (2012).

32. Paxinos, G. & Franklin, K. B. J. Paxinos and Franklin's the Mouse Brain in Stereotaxic Coordinates. (Academic Press, 2019).

Acknowledgements

We thank Ravi Tolwani and the staff of the Comparative Biosciences Center, Connie Zhao and the staff of the Genomics Resource Center, Alison North and the staff of the Bioimaging Resource Center at Rockefeller University for technical assistance. We thank Alexander Nectow for the AAV-Introvert-GFPL10a virus and David Anderson for providing the HSV-lsl-tdTomato virus. We thank Christin Kosse for providing MATLAB codes for photometry analysis. This work was funded by a Long Term HSFP Fellowship (E.P.A.), F32DK107077 (S.A.S.), NARSAD Young Investigator Awards from the Brain and Behavior Research Foundation (E.P.A and S.A.S) the JPB Foundation and the Klarman Foundation (J.M.F).

Author Contributions:

E.P.A and S.A.S conceived the study, designed and conducted the experiments and analyzed data. K.R.D. assisted with immunohistochemistry, B.T. assisted with RNAscope, L.E.P. conducted anterograde and rabies tracing, M.S. assisted with feeding studies. R.N.F. and C.L assisted with the analysis of fiber photometry and provided custom-written MATLAB codes. S.A.S, E.P.A and J.M.F secured funding and wrote the manuscript with

the input of all authors.

Data availability

The data that support the findings of this study are available from the corresponding author upon reasonable request.

Code availability

The custom codes used in this study are available from the corresponding author upon reasonable request.

Competing interests

The authors declare no competing interests.

Correspondence and requests for materials should be addressed to friedj@mail.rockefeller.edu or to sstern01@rockefeller.edu

Fig 1

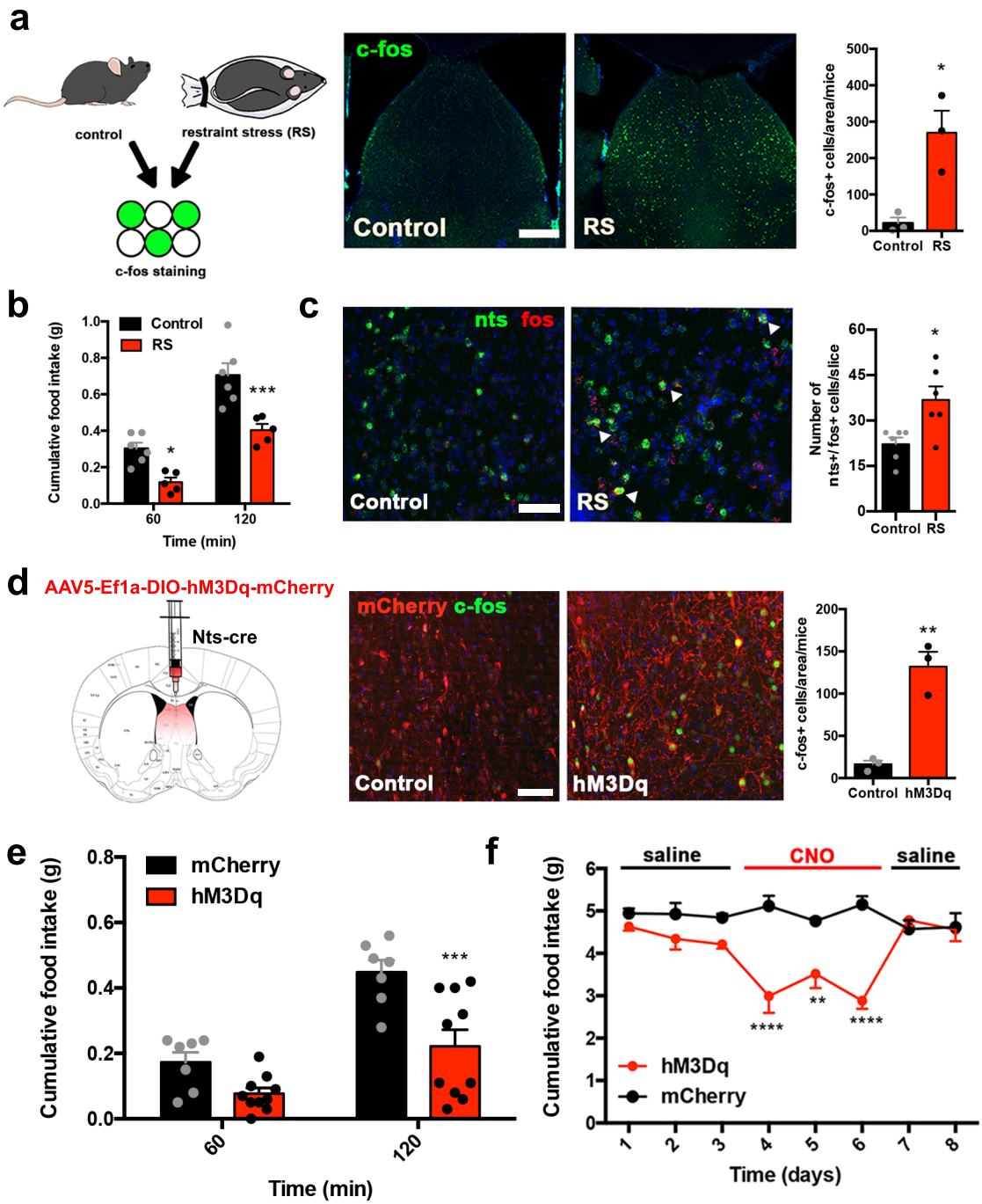

Figure 1. Nts^{LS} neurons respond to stress and are anorexigenic. a, Left, experimental scheme in which c-fos+ cells were quantified in the LS following restraint stress. Middle, representative images of c-fos (green) in control and restraint stress (RS) mice. Right, quantification of c-fos+ cells in control (black) and RS (red) mice. n= 3, unpaired Students' t-test p=0.02, t(4)=3.964. b, Food intake, measured in grams (g), in control (black) and RS (red) mice 1 hour and 2 hours following RS. n=5 (RS), n=6(control),Two-way ANOVA with post-hoc Bonferroni correction (Time: F(1,9)=175.9, p<0.0001; Subject:F(1,9)=16.86, p=0.003; Interaction: F(1,9)=4.975, p=ns). c, Left, representative in situ hybridization images of nts (green) and fos (red) in control (left) and RS (right). White arrows point to nts/fos colocalized cells. DAPI is in blue. Right, quantification of nts+/fos+ cells in control (black) and RS (red) mice. n=6, unpaired Students' t-test, t(10)=2.962, p=0.01. d, Left, experimental scheme. Nts-cre mice were injected with an AAV encoding the hM3Dq activatory DREADD receptor in the LS. Middle, representative images of viral expression (mCherry, red) and cfos (green) in control virus (left) and hM3Dq (right) injected mice following CNO injection. Right, quantification of c-fos+ cells in mCherry control (black) and hM3Dq (red) expressing mice. n=3, unpaired Students' t-test, p=0.003, t(4)=6.418. e, Food intake, measured in grams (g) of control mCherry (black) and hM3Dq (red) expressing Nts-cre mice following CNO injection. n=7(mCherry), n=10(hM3Dq), Two-way ANOVA with post-hoc Bonferroni correction (Time: F(1,15)=55.46, p<0.0001; Subject: F(1,15)=12.84, p=0.0027; Interaction: F(1,15)=5.45, p=0.034).f, Food intake, measured in grams (g) during days with daily saline (days 1-3, 7-8) or CNO (days 4-6) injection in control mCherry (black) or hM3Dq (red) expressing Nts-cre mice. n=8; Two-way ANOVA with post-hoc Bonferroni correction. (Time: F(7,72)=2.871, p=0.01; Subject: F(1,72)=46.92, p<0.0001; Interaction: F(7,72)=6.48, p<0.0001). The mouse brain in this and subsequent figures was reproduced with permission from Paxinos and Franklin[32], copyright 2012. Data are represented as mean +- SEM. *P<0.05, **P<0.01

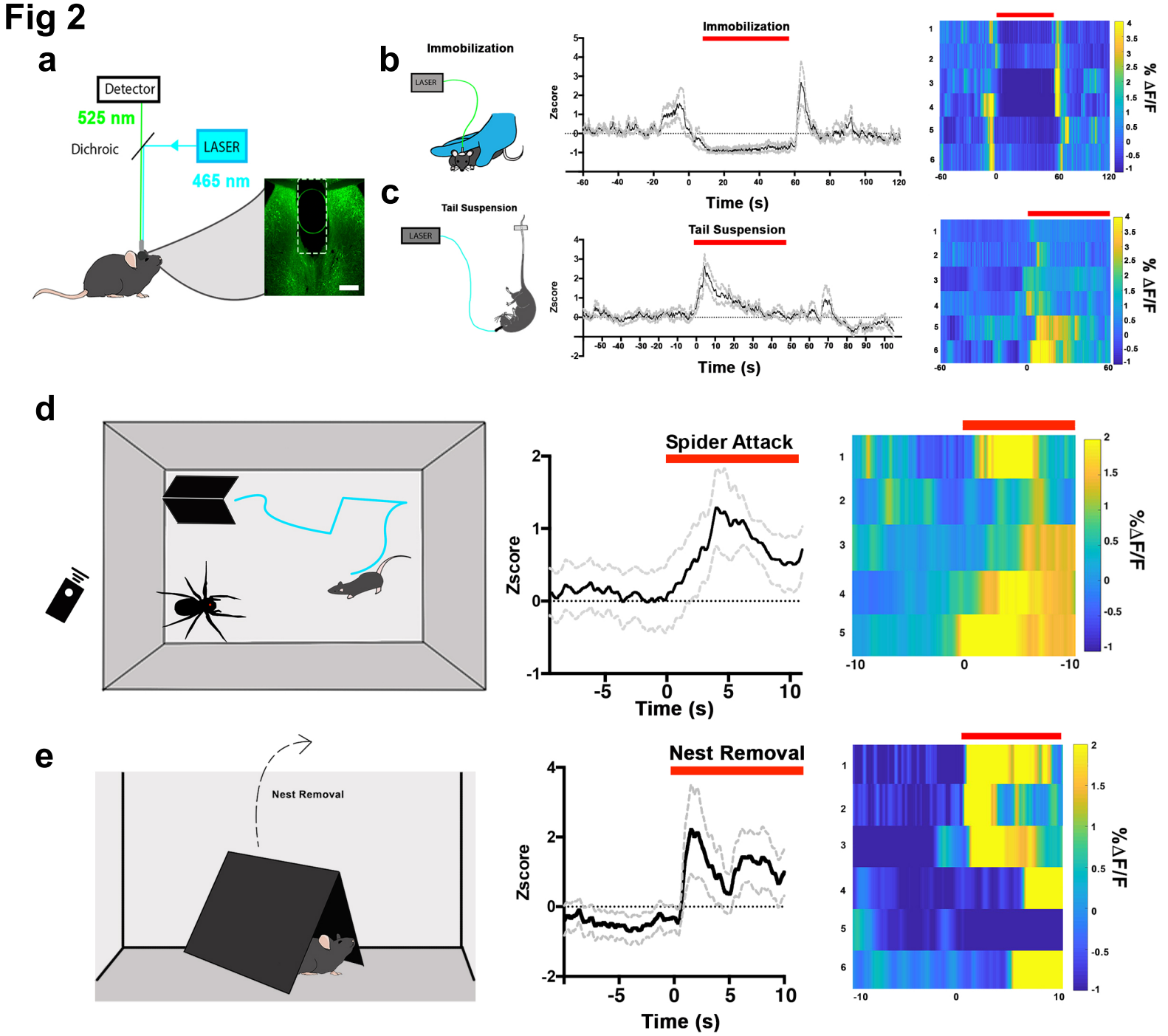

Figure 2. Nts^{LS} neurons are specifically activated during predator-induced stress. a, Experimental scheme and representative image of the LS of Nts-cre mice injected with GCaMP6s and implanted with an optic fiber in the LS. Mice were then attached to a fiber photometry setup with a 465nm LED (blue) and a 405 nm LED (purple) and a photodetector. b, Left, experimental scheme. Ca+2 activity was recorded during 5 minutes of manual restraint stress. Middle, Average GCaMP6s z-score (black lines) and SEM (gray dotted lines) across all recording sites time-locked to restraint stress start. Right, Heat maps represent the average % ΔF/F from each GCaMP6s recordings time-locked to restraint stress start. n=6. c, Left, experimental scheme. Ca+2 activity was recorded during a 5-minute tail suspension. Middle, Average GCaMP6s z-score (black lines) and SEM (gray dotted lines) across all recording sites time-locked to tail suspension stress start. Right, Heat maps represent the average % ΔF/F from each GCaMP6s recordings time-locked to tail suspension stress start. n=6. d, Left, experimental scheme. Ca+2 activity was recorded in an open field that contained a remote-controlled spider and a designated safe "nest" (black triangular hut). Middle, Average GCaMP6s z-score (black lines) and SEM (gray dotted lines) across all recording sites time-locked to the start of the first spider attack. Right, Heat maps represent the average % ΔF/F from each GCaMP6s recordings time-locked to the start of the spider attack. n=5. e, Left, experimental scheme. Ca+2 activity was recorded in an open field that contained a remote-controlled spider and a designated safe "nest" (black triangular hut). During the experiment, the safe "nest" was removed. Middle, Average GCaMP6s z-score (black lines) and SEM (gray dotted lines) across all recording sites time-locked to the removal of the safe "nest". Right, Heat maps represent the average % ΔF/F from each GCaMP6s recordings time-locked to the removal of the safe "nest". n=6.

Fig 3

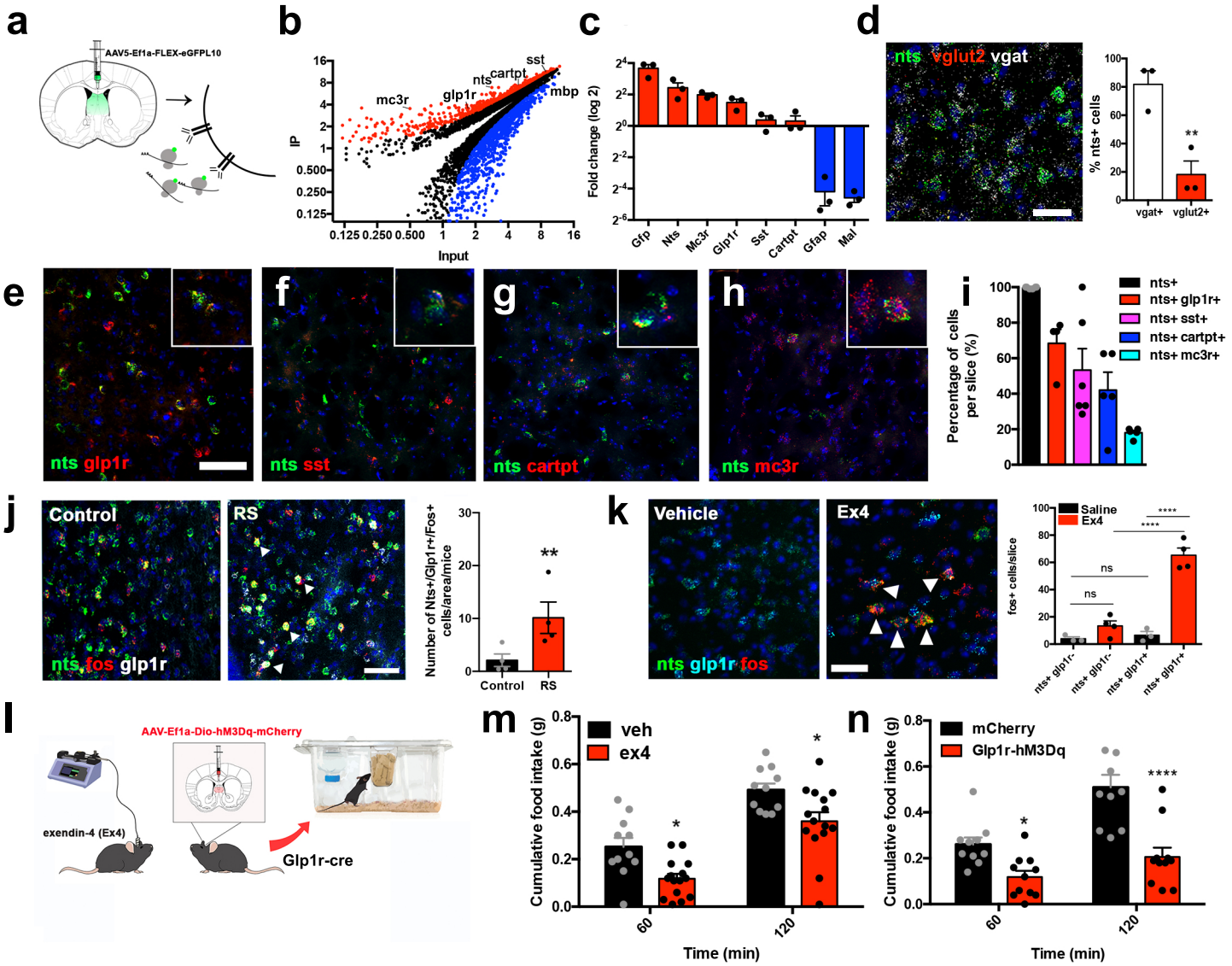

Figure 3. Nts^{LS} neurons co-express Glp1r to regulate feeding. a, Experimental scheme of viral-trap experiment. Nts-cre mice are injected with an AAV expressing cre-dependent GFPL10 (AAV-Eef1a-FLEX-eGFPL10) into the LS and then GFP+ polysomes are immunoprecipitated. b, Plot depicting the average IP value and average input values (log2) of all genes analyzed. Enriched genes (>2-fold; red) and depleted genes (<2-fold; blue) are shown (q<0.05), and selected markers are shown: mc3r, glp1r, nts, cartpt and mbp (n = 3 biological replicates). All genes depicted have q values <0.05 as calculated by Cufflinks. c, Average fold of change (IP/INP Log2) assessed by qPCR of enriched positive control markers gfp and nts, significantly enriched genes mc3r, glp1r, sst and cartpt (red) and depleted negative control markers gfap and mal (blue) (n = 3 biological replicates). d, Left, representative in situ hybridization image of nts (green), vglut2 (red), vgat (white) and DAPI (blue). Right, quantification of nts cells which express vgat (white) and vglut2 (red). n=3, Students' t-test p=0.009; t(4)=4.791 e, Representative in situ hybridization image of nts (green) and glp1r (red). Closer magnification is inset. f, Representative in situ hybridization image of nts (green) and sst (red). Closer magnification is inset. g, Representative in situ hybridization image of nts (green) and cartpt (red). Closer magnification is inset. h, Representative in situ hybridization image of nts (green) and mc3r (red). Closer magnification is inset. i, Quantification of the percentage of nts cells (black) expressing nts/glp1r (red), sst (magenta), cartpt (blue) and mc3r (cyan). n=3(nts), n=4(nts/glp1r, Nts/mc3r), n=6(nts/sst), n=5(nts/cartpt). j, Representative images of nts (green), fos (red) and glp1r (white) in control and restraint stress (RS) mice. Right, quantification of co-localization between nts, fos and glp1r+ cells in control (black) and RS (red) mice. n= 4, Nested t-test p=0.0056, t(8)=3.75. Scale bars, 50 μm. k, Left, representative in situ hybridization image of nts (green), glp1r (blue) and fos (red) of mice injected with vehicle or the Glp1r agonist Exendin-4 (Ex4). White arrows point to cells co-expressing nts, glp1r and fos. Right, quantification of fos+ cells expressing nts and/or glp1r in saline (black) or Ex4 (red) injected mice. n=3(Control), n=4 (Ex4); Two-way ANOVA with Bonferroni correction (Subject: F(1,10)=71.7, p<0.0001; Treatment: F(1,10)=45,88, p=0.0001; Interaction: F(1,10)=37.58, p<0.0001). Scale bars, 30 μm. i, Experimental scheme. Wild-type mice are injected with Ex4 directly into the LS or Glp1r-cre mice with viral expression of hM3Dq activatory DREADD receptor are tested for cumulative food intake. m, Food intake, measured in grams (g) of mice following Vehicle (black) and Ex4 (red) injection in the LS. n=11(Vehicle), n=15(Ex4), Two-way ANOVA with post-hoc Bonferroni correction (Time: F(1,24)=100.8, p<0.0001; Treatment: F(1,24)=11.54, p=0.0024; Interaction: F(1,24)=0.002; p=0.963. n, Food intake, measured in grams (g) of control mCherry (black) and hM3Dq (red) expressing Glp1r-cre mice following CNO injection. Two-way ANOVA with post-hoc Bonferroni correction. n=10(mCherry), n=11(hM3Dq). (Time: F(1,19)=40,67, p<0.0001; Subject: F(1,19)=20.68, p=0.0002; Interaction: F(1,19)=9,407, p=0.0063. Data are represented as mean +- SEM. *P<0.05, **P<0.01, ****P<0.0001.

Fig 4

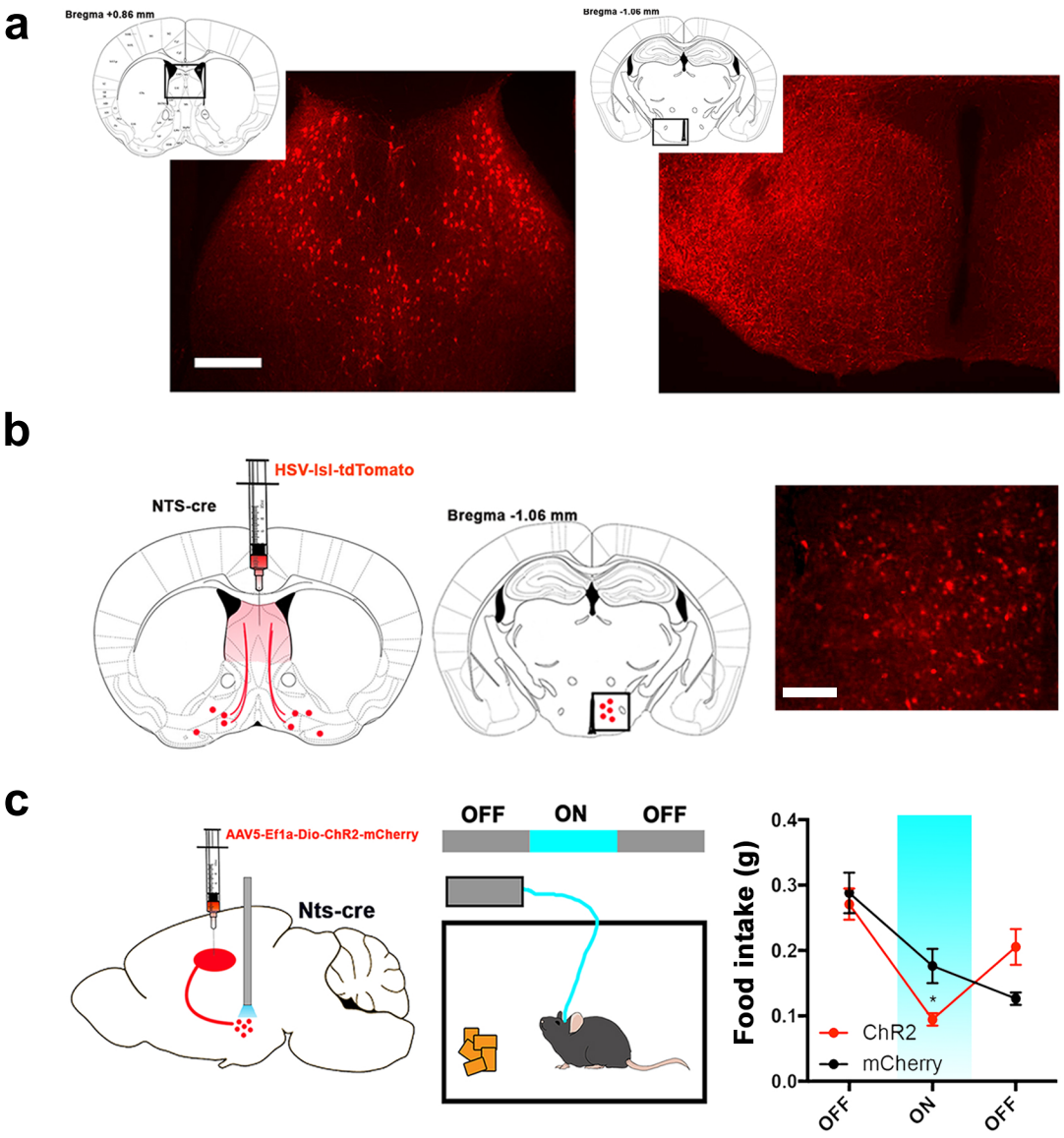

Figure 4. An LH projection mediates anorexia induced by Nts^{LS} neurons. a, Representative images of the LS injection site (left) and terminals in the lateralhypothalamus (left) of Nts-cre mice injected with a control mCherry reporter virus. Atlas images above the representative images depict the area of magnification. b, Representative image of cells labeled in the lateral hypothalamus (right) of Nts-cre mice injected with the anterograde tracer HSV-lsl-tdTomato in the LS. Middle, atlas image depicting the area of magnification to the right. c, Left, experimental scheme depicting mice injected with AAV expressing Chr2 or control mCherry into the LS and an optic fiber positioned over the lateral hypothalamus. Middle, food intake was measured in an OFF-ON-OFF paradigm. Right, food intake measured in grams (g) of control mCherry (black) or Chr2 (red) expressing mice before (OFF), during (ON) and after (OFF) laser stimulation. n=11, Two-way ANOVA with post-hoc Bonferroni correction (Epoch: $F(2,40)=38.47$, $p<0.0001$; Subject: $F(1,20)=0.069$, $p=0.796$; Interaction: $F(2,40)=10.94$, $p=0.0002$. Data are represented as mean +- SEM.